Advances in Chemical Physics
Stuart A. Rice and Aaron R. Dinner, Series Editors

Advances in Chemical Physics

Volume 160

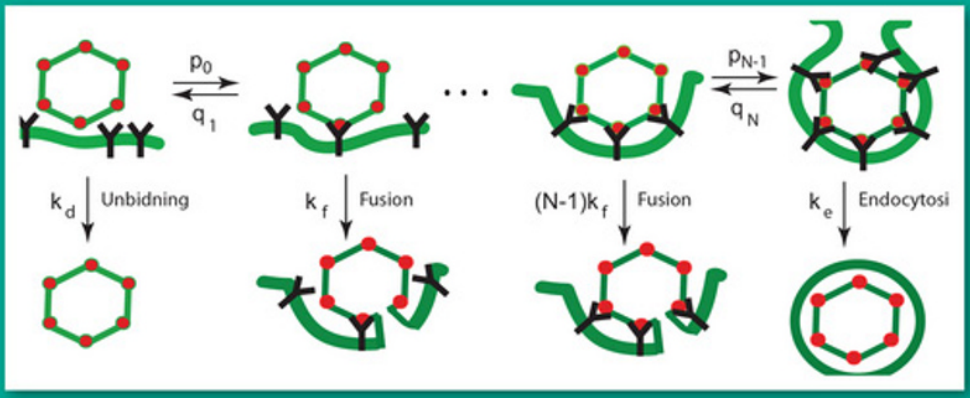

Edited by
Stuart A. Rice and Aaron R. Dinner

WILEY

ADVANCES IN CHEMICAL PHYSICS

VOLUME 160

ADVANCES IN CHEMICAL PHYSICS

VOLUME 160

Series Editors

STUART A. RICE

Department of Chemistry
and
The James Franck Institute,
The University of Chicago,
Chicago, IL, USA

AARON R. DINNER

Department of Chemistry
and
The James Franck Institute,
The University of Chicago,
Chicago, IL, USA

WILEY

Published by John Wiley & Sons, Inc., Hoboken, New Jersey
Published simultaneously in Canada

Library of Congress Catalog Number: 58-9935

ISBN: 9781119165149

Set in 10/12pt Times by SPi Global, Pondicherry, India

Printed in the United States of America

10 9 8 7 6 5 4 3 2 1

EDITORIAL BOARD

CONTENTS

Contributors List ix
Preface to the Series xi

Thermodynamic Perturbation Theory for Associating Molecules 1

Bennett D. Marshall and Walter G. Chapman

Path Integrals and Effective Potentials in the Study of Monatomic Fluids at Equilibrium 49

Luis M. Sesé

Spontaneous Symmetry Breaking in Matter Induced by Degeneracies and Pseudodegeneracies 159

Isaac B. Bersuker

Mean Field Electrostatics Beyond the Point Charge Description 209

Derek Frydel

First-Passage Processes in Cellular Biology 261

Srividya Iyer-Biswas and Anton Zilman

Theoretical Modeling of Vibrational Spectra and Proton Tunneling in Hydrogen-Bonded Systems 307

Marek Janusz Wójcik

Index 343

CONTRIBUTORS LIST

BENNETT D. MARSHALL, ExxonMobil Research and Engineering, Spring, TX, USA

WALTER G. CHAPMAN, Department of Chemical and Biomolecular Engineering, Rice University, Houston, TX, USA

LUIS M. SESÉ, Departamento de Ciencias y Técnicas Fisicoquímicas, Universidad Nacional de Educación a Distancia, Madrid, Spain

ISAAC B. BERSUKER, Institute for Theoretical Chemistry, Department of Chemistry, University of Texas at Austin, Austin, TX, USA

DEREK FRYDEL, Institute for Advanced Study, Shenzhen University, Shenzhen, China; School of Chemistry and Chemical Engineering, Shanghai Jiao Tong University, Shanghai, China; Laboratoire de Physico-Chime Thèorique, ESPCI, CNRS Gulliver, Paris, France

SRIVIDYA IYER-BISWAS, Department of Physics and Astronomy, Purdue University, West Lafayette, IN 47907, USA

ANTON ZILMAN, Department of Physics and Institute for Biomaterials and Biomedical Engineering, University of Toronto, Toronto, Ontario, Canada

MAREK JANUSZ WÓJCIK, Faculty of Chemistry, Jagiellonian University, Kraków, Poland

PREFACE TO THE SERIES

Advances in science often involve initial development of individual specialized fields of study within traditional disciplines followed by broadening and overlap, or even merging, of those specialized fields, leading to a blurring of the lines between traditional disciplines. The pace of that blurring has accelerated in the past few decades, and much of the important and exciting research carried out today seeks to synthesize elements from different fields of knowledge. Examples of such research areas include biophysics and studies of nanostructured materials. As the study of the forces that govern the structure and dynamics of molecular systems, chemical physics encompasses these and many other emerging research directions. Unfortunately, the flood of scientific literature has been accompanied by losses in the shared vocabulary and approaches of the traditional disciplines, and there is much pressure from scientific journals to be ever more concise in the descriptions of studies, to the point that much valuable experience, if recorded at all, is hidden in supplements and dissipated with time. These trends in science and publishing make this series, *Advances in Chemical Physics*, a much needed resource.

The *Advances in Chemical Physics* is devoted to helping the reader obtain general information about a wide variety of topics in chemical physics: a field that we interpret very broadly. Our intent is to have experts present comprehensive analyses of subjects of interest and to encourage the expression of individual points of view. We hope that this approach to the presentation of an overview of a subject will both stimulate new research and serve as a personalized learning text for beginners in a field.

STUART A. RICE
AARON R. DINNER

THERMODYNAMIC PERTURBATION THEORY FOR ASSOCIATING MOLECULES

BENNETT D. MARSHALL[1] and WALTER G. CHAPMAN[2]

[1]*ExxonMobil Research and Engineering, Spring, TX, USA*
[2]*Department of Chemical and Biomolecular Engineering, Rice University, Houston, TX, USA*

CONTENTS

I. Introduction
II. A Brief Introduction to Cluster Expansions
III. Single Association Site: Bond Renormalization
IV. Single Association Site: Two-Density Approach
  A. The Monovalent Case
  B. The Divalent Case
V. Multiple Association Sites: Multi-Density Approach
VI. The Two-Site AB Case
  A. Steric Hindrance in Chain Formation
  B. Ring Formation
  C. Bond Cooperativity
VII. Spherically Symmetric and Directional Association Sites
VIII. Density Functional Theory
IX. Concluding Remarks
Acknowledgments
References

I. INTRODUCTION

Since the time of van der Waals, scientists have sought to describe the macroscopic behavior of fluids in terms of the microscopic interactions of the constituent molecules. By the early 1980s, accurate theories based on statistical mechanics had primarily been developed for near-spherical molecules. Successes of the 1960s and 1970s particularly by Chandler, Weeks, and Andersen [1] and by Barker and Henderson [2] produced perturbation theories for the properties of Lennard-Jones (LJ) fluids. Site–site theories such as reference interaction site model (RISM) [3] were developed,

Advances in Chemical Physics, *Volume 160*, First Edition. Stuart A. Rice and Aaron R. Dinner.

in part, to provide reference fluid structure to extend these perturbation theories to polyatomic molecules. However, for certain classes of fluids, the accurate description of the fluid phase in terms of the microscopic interactions has proven much more challenging. Hydrogen bonding interactions are strong, short-ranged, highly directional interactions that lie somewhere between a dipole/dipole attraction and a covalent bond. The short range and directionality of hydrogen bonds result in the phenomena of bond saturation, giving a limited valence of the hydrogen bonding attractions.

The same properties of the hydrogen bond, which complicate the theoretical description of these fluids, also give rise to a number of macroscopic physical properties that are unique to fluids that exhibit hydrogen bonding. Hydrogen bonding is responsible for the remarkable properties of water [4], folding of proteins [5] and is commonly exploited in the self-assembly [6] of advanced materials. More recently patchy colloids, a new class of materials that shares many qualities with hydrogen bonding fluids, have been developed. Patchy colloids are colloids with some number of attractive surface patches giving rise to association like anisotropic inter-colloid potentials [7]. For the purposes of this review, patchy colloids and hydrogen bonding fluids are treated on equal footing and will simply be termed "associating fluids."

The first models used to describe hydrogen bonding fluids were developed using a chemical approach, where each associated cluster is treated as a distinct species created from the reaction of monomers and smaller associated clusters [8, 9]. The "reactions" are governed by equilibrium constants that must be obtained empirically. This type of approach has been incorporated into various equations of state including a van-der-Waals-type equation of state [10], the perturbed anisotropic chain theory equation of state (APACT) [11], and the Sanchez–Lacombe [12] equation of state.

Alternatively, lattice theories may be employed to model hydrogen bonding fluids. These approaches generally follow the method of Veytsman [13] who showed how the free energy contribution due to hydrogen bonding could be calculated in the mean field by enumerating the number of hydrogen bonding states on a lattice. Veytsman's approach was incorporated into the Sanchez–Lacombe equation of state by Panayiotou and Sanchez [14] who factored the partition function into a hydrogen bonding contribution and a non-hydrogen bonding contribution. The lattice approach has also been applied to hydrogen bond cooperativity [15] and intramolecular [16] hydrogen bonds.

Both the chemical and lattice theory approaches to hydrogen bonding yield semi-empirical equations of state, which are useful for several hydrogen bonding systems [8]. The drawback of these approaches is a result of their simplistic development. As discussed earlier, it is desired to describe the macroscopic behavior of fluids through knowledge of the microscopic intermolecular interactions and distributions. This cannot be accomplished using a lattice or chemical theory. To accomplish this goal, we must incorporate molecular details of the associating fluid from the outset.

The starting place for any molecular theory of association is the definition of the pair potential energy $\phi(12)$ between molecules (or colloids). Molecules are treated as rigid bodies with no internal degrees of freedom. In total, six degrees of freedom describe any single molecule: three translational coordinates represented by the vector $\vec{r}_1$ and three orientation angles represented by Ω_1. These six degrees of freedom are represented as $1 = \{\vec{r}_1, \Omega_1\}$. It is assumed that the intermolecular potential can be separated as

$$\phi(12) = \phi_{ref}(12) + \phi_{as}(12) \tag{1}$$

where $\phi_{as}(12)$ contains the association portion of the potential and $\phi_{ref}(12)$ is the reference system potential, which contains all other contributions of the pair potential including a harsh short-ranged repulsive contribution.

Considering molecules (or colloids) that have a set of association sites $\Gamma = \{A, B, C, \ldots, Z\}$, where association sites are represented by capital letters, the association potential is decomposed into individual site–site contributions

$$\phi_{as}(12) = \sum_{A\in\Gamma}\sum_{B\in\Gamma}\phi_{AB}(12) \tag{2}$$

The potential $\phi_{AB}(12)$ represents the association interaction between site A on molecule 1 and site B on molecule 2. One of the challenges in developing theoretical models for associating fluids stems from the short-ranged and directional nature of the association potential ϕ_{AB}, which results in the phenomena of bond saturation. For instance, considering molecules which consist of a hard spherical core of diameter d

$$\phi_{ref}(12) = \phi_{HS}(r_{12}) = \begin{cases} \infty & r < d \\ 0 & r \geq d \end{cases} \tag{3}$$

and a single association site A (see Fig. 1), bond saturation arises as follows. When spheres 1 and 2 are positioned and oriented correctly such that an association bond is formed, the hard cores of these two spheres may, depending on the

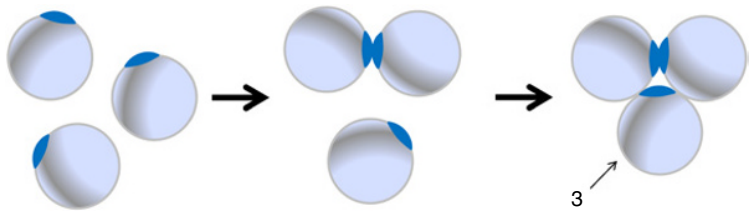

Figure 1. Illustration of bond saturation for hard spheres with a single monovalent association site. (*See insert for color representation of the figure.*)

size and range of the association site, prevent sphere 3 from approaching and sharing in the association interaction. That is, if $\phi_{as}(12) < 0$ and $\phi_{as}(13) < 0$, then $\phi_{HS}(r_{23}) = \infty$, meaning that each association site is singly bondable (has a valence of 1). In hydrogen bonding it is usually the case that each association bond site is singly bondable, although there are exceptions. For the case of patchy colloids, the patch size can be controlled to yield a defined valence controlling the type of self-assembled structures that form.

Conical square well (CSW) association sites are commonly used as a primitive model for the association potential ϕ_{AB}. First introduced by Bol [17] and later reintroduced by Chapman *et al.* [18, 19], CSWs consider association as a square well interaction which depends on the position and orientation of each molecule. Kern and Frenkel [20] later realized that this potential could describe the interaction between patchy colloids. For these CSWs the association potential is given by

$$\begin{aligned} \phi_{AB}(12) &= -\varepsilon_{AB} \mathrm{O}_{AB}(12) \\ \mathrm{O}_{AB}(12) &= \begin{cases} 1, & r_{12} \le r_c ; \theta_{A1} \le \theta_c ; \theta_{B2} \le \theta_c \\ 0 & \text{otherwise} \end{cases} \\ f_{AB}(12) &= \left(\exp\left(\varepsilon_{AB}/\mathrm{k_{bT}}\right) - 1\right) \mathrm{O}_{AB}(12) = f_{AB} \mathrm{O}_{AB}(12) \end{aligned} \tag{4}$$

where r_c is the maximum separation between two colloids for which association can occur, θ_{A1} is the angle between $\vec{r}_{12}$ and the orientation vector passing through the center of the patch on colloid 1, and θ_c is the critical angle beyond which association cannot occur. Equation (4) states that if the spheres are close enough $r_{12} < r_c$, and both are oriented correctly $\theta_{A1} < \theta_c$ and $\theta_{B2} < \theta_c$, then an association bond is formed and the energy of the system is decreased by ε_{AB}. Figure 2 gives an illustration of two single-site spheres interacting with this potential. The size of the patch is dictated by the critical angle θ_c that defines the solid angle to be $2\pi\,(1 - \cos\theta_c)$. The patch size determines the maximum number of other spheres to which the patch can bond. Specifically considering a hard sphere reference fluid with association occurring at hard sphere contact $r_c = d$, it is possible for a

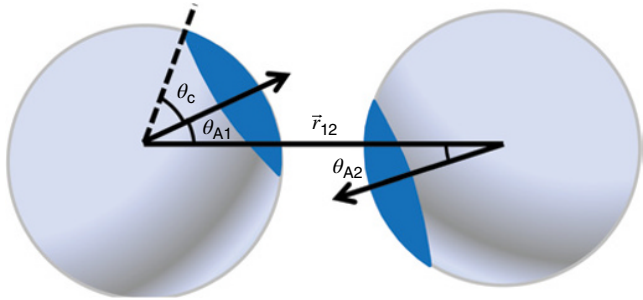

Figure 2. Association parameters for conical association sites. (*See insert for color representation of the figure.*)

patch to associate at most once for $0^\circ \le \theta_c < 30^\circ$, twice for $30^\circ \le \theta_c < 35.3^\circ$, thrice for $35.3^\circ \le \theta_c < 45^\circ$, and four times for $45^\circ \le \theta_c < 58.3^\circ$ [21]. The advantage of the CSW model is that it separates the radial and angular dependence of the potential and allows for analytic calculations in the model while allowing for quick calculation of association in a simulation since only two dot products are needed to determine that the molecular orientation criteria is satisfied for association.

In the following sections we review some of the existing theories to model associating fluids with potentials of the form of Eqs. (1)–(2). We focus mainly on the multi-density formalism of Wertheim [22, 23], which has been widely applied across academia and industry. In Sections III and IV.A, only association sites that are singly bondable are considered and steric hindrance between association sites is neglected. Extensions of Wertheim's multi-density approach for the divalent case is described in Section IV.B. Section V addresses the case of multiple association sites on a molecule within Wertheim's multi-density formalism. Section VI extends the theory to the case of a small angle between two association sites, so that the sites cannot be assumed to be independent, and for the case of cooperative hydrogen bonding. Section VII extends the theory to account for association interactions between molecules with spherically symmetric and directional association sites (e.g., ion–water solvation). A brief description of applying the density functional theory (DFT) approach for associating molecules is presented in Section VIII. Finally, Section IX gives concluding remarks. Prior to exploring the theory, a brief introduction to cluster expansions is provided in Section II.

II. A BRIEF INTRODUCTION TO CLUSTER EXPANSIONS

In this section we give a very brief overview of cluster expansions. For a more detailed introduction the reader is referred to the original work of Morita and Hiroike [24] and also to the reviews by Stell [25] and Andersen [26]. Cluster expansions were first introduced by Mayer [27] as a means to describe the structure and thermodynamics of non-ideal gases. In cluster expansions Mayer f functions are introduced:

$$f(12) = \exp\left(\frac{-\phi(12)}{k_B T}\right) - 1 \tag{5}$$

The replacement $\exp(-\phi(12)/k_B T) = f(12) + 1$ in the grand partition function and the application of the lemmas developed by Morita and Hiroike [24] allows for the pair correlation function $g(12)$ and Helmholtz free energy A to be written as an infinite series in density where each contribution is an integral represented pictorially by a graph. A graph is a collection of black circles and white circles with bonds connecting some of these circles. The bonds are represented by

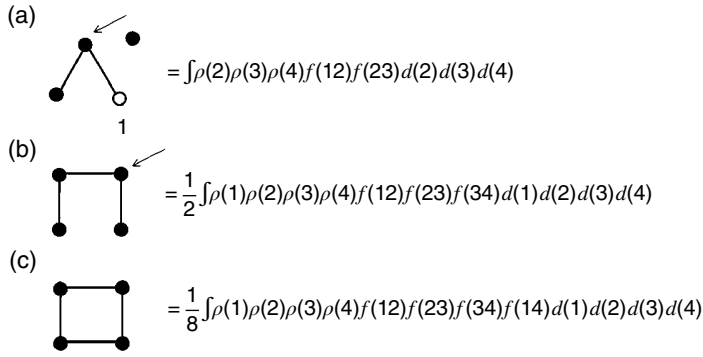

Figure 3. Examples of integral representations of graphs. Arrows point towards articulation circles.

two-molecule functions such as Mayer functions $f(12)$ and the black circles are called "field points" represented by single-molecule functions such as fugacity $z(1)$ or density $\rho(1)$ integrated over the coordinates (1). The white circles are called "root points" and are not associated with a single-molecule function, and the coordinates of a root point are not integrated. Root points are given labels 1, 2, 3,…. The value of the diagram is then obtained by integrating over all coordinates associated with field points and multiplying this integral by the inverse of the symmetry number S of the graph. Figure 3 gives several examples. The volume element $d(1)$ is given by $d(1) = d\vec{r}_1 d\Omega_1$, representing the differential position and orientation of the molecule.

Before giving graphical representations of the pair correlation function $g(12)$ and the Helmholtz free energy A, a few definitions must be given as follows:

1. A graph is connected if there is at least one path between any two points. Graph **a** in Fig. 3 is disconnected, and graphs **b** and **c** are both connected.
2. An articulation circle is a circle in a connected graph whose removal makes the graph disconnected, where at least one part contains no root point and at least one field point Arrows in Fig. 3 point to articulation circles.
3. An irreducible graph has no articulation circles. Graph **c** in Fig. 3 is an example of an irreducible graph.

Using these definitions, the pair correlation function and Helmholtz free energy are given as

$$g(12) = \left\{ \begin{array}{l} \text{sum of topologically different irreducible graphs that have two root} \\ \text{points labelled 1 and 2, any number of field points } \rho, \text{ and at most} \\ \text{one } f \text{ bond between each pair of points} \end{array} \right\} \tag{6}$$

and

$$\frac{A}{k_B T} = \int \rho(1)\left(\ln\left(\rho(1)\Lambda^3\right) - 1\right) d(1) - c^{(o)} \tag{7}$$

where Λ is the de Broglie wavelength, $\rho(1)$ is the density where $\rho(\vec{r}) = \int \rho(1)\, d\Omega$, and $c^{(o)}$ is the graph sum given by

$$c^{(o)} = \left\{ \begin{array}{l} \text{sum of topologically different irreducible graphs that have no root} \\ \text{points any number of field points } \rho, \text{ and at most one } f \text{ bond between} \\ \text{each pair of points} \end{array} \right\} \tag{8}$$

Equations (6)–(8) are rigorous and exact mathematical statements. Unfortunately, the exact evaluation of these infinite sums cannot be performed and numerous approximations must be made to obtain any usable result. In these approximations only some subset of the original graph sum is evaluated.

Performing these partial summations in hydrogen bonding fluids is complicated by both the strength of the association interaction and the limited valence of the interaction. Hydrogen bond strengths can be many times that of typical van der Waals forces giving Mayer functions which are very large. If the entire cluster series were evaluated for $g(12)$ and $c^{(o)}$ many of these large terms would cancel; however, when performing partial summations, care must be taken to eliminate divergences if meaningful results are to be obtained. Similarly, in most hydrogen bonding fluids, each hydrogen bonding group is singly bondable. Hence, any theory for hydrogen bonding fluids must account for the limited valence of the attractions. Again, if the full cluster series were evaluated for $g(12)$ this condition would be naturally accounted for; however, when performing partial summations care must be taken to ensure this single bonding condition holds. There have been three general methods to handle these strong association interactions using cluster expansions. The first was the pioneering work of Andersen [28, 29] who developed a cluster expansion for associating fluids in which the divergence was tamed by the introduction of renormalized bonds, the second is the approach of Chandler and Pratt [30] who used physical clusters to represent associated molecules, and the third is the method of Wertheim [22, 23, 31–33] who used multiple densities. Both Andersen and Wertheim took the approach of incorporating the effects of steric hindrance early in the theoretical development in the form of mathematical clusters. In what follows, for brevity, we restrict our attention to the approaches of Andersen and Wertheim, however, when possible we draw parallels between these approaches and that of Chandler and Pratt.

III. SINGLE ASSOCIATION SITE: BOND RENORMALIZATION

Before discussing the more general case of associating fluids with multiple association sites, we will discuss the simpler case of molecules with a single association site A. For a single association site, the Mayer function is decomposed as

$$f(12) = f_{ref}(12) + F_{AA}(12) \tag{9}$$

where

$$\begin{aligned} F_{AA}(12) &= e_{ref}(12) f_{AA}(12) \\ e_{ref}(12) &= \exp\left(\frac{-\phi_{ref}(12)}{k_B T}\right) = 1 + f_{ref}(12) \\ f_{AA}(12) &= \exp\left(\frac{-\phi_{AA}(12)}{k_B T}\right) - 1 \end{aligned} \tag{10}$$

In Eq. (10) the $f_{AA}(12)$ accounts for the anisotropic/short-ranged attraction of the association interaction and the function $e_{ref}(12)$ prevents the overlap of the cores of the molecules. It is the functions $e_{ref}(12)$ that give rise to the single bonding condition. Now inserting Eq. (9) into Eq. (6) and simplifying

$$g(12) = \left\{ \begin{array}{l} \text{sum of topologically different irreducible graphs that have two} \\ \text{root points labelled 1 and 2, any number of field points } \rho, f_{ref} \text{ and} \\ F_{AA} \text{ bonds, and at most one bond between each pair of points} \end{array} \right\} \tag{11}$$

Andersen [28, 29] defines a renormalized association Mayer function $\tilde{F}_{AA}(12)$ as the sum of the graphs in Eq. (11) which are most important in the determination of $g(12)$. Since the Mayer functions F_{AA} may take on very large numerical values in the bonding region, the most important graphs in the calculation of $g(12)$ are the ones whose root points are connected by an F_{AA} bond. Hence, it is natural to define $\tilde{F}_{AA}$ as

$$\tilde{F}_{AA}(12) = \left\{ \begin{array}{l} \text{sum of graphs in } (11) \text{ whose root points are connected} \\ \text{by an } F_{AA} \text{ bond} \end{array} \right\} \tag{12}$$

Andersen assumes that the intermolecular potential was such that the association site was singly bondable. This single bonding condition was exploited in the

cluster expansion by use of the *cancelation theorem* as described by Andersen, who was able to sum the diagrams in Eq. (12) as

$$\tilde{F}_{AA}(12) = F_{AA}(12) Y_p(12) \frac{1 + 2\Delta_{AA} - \sqrt{1 + 4\Delta_{AA}}}{2\Delta_{AA}^2} \tag{13}$$

where the term Δ_{CD} is given by (where for a homogeneous fluid $\rho = \int \rho(1)\, d\Omega_1$)

$$\Delta_{CD} = \frac{\rho}{\Omega} \int Y_p(12) F_{CD}(12) d(2) \tag{14}$$

and $\Omega = \int d\Omega'$ is the total number of orientations. The function $Y_p(12)$ is given by

$$Y_p(12) = \left\{ \begin{array}{l} \text{sum of graphs in } (11) \text{ which have no } F_{AA} \text{ bond attached} \\ \text{to either root, and no bond between the roots} \end{array} \right\} \tag{15}$$

It is easily shown that $\tilde{F}_{AA}(12)$ is bounded as follows:

$$0 \le \frac{\rho}{\Omega} \int \tilde{F}_{AA}(12) d(2) \le 1 \tag{16}$$

Equation (16) shows that the renormalized association bond remains finite even when the association potential ϕ_{AA} takes on infinitely large negative values. Using this renormalized bond the average number of hydrogen bonds per molecule is calculated as follows:

$$N_{HB} = \frac{\rho}{\Omega} \int \tilde{F}_{AA}(12) d(2) \tag{17}$$

Comparing Eqs. (16) and (17) it is easy to see

$$0 \le N_{HB} \le 1 \tag{18}$$

Equation (18) demonstrates that the single bonding condition is satisfied and that the method of Andersen was successful. Unfortunately, the function $Y_p(12)$ must be obtained through the solution of a series of integral equations using approximate closures.

To the author's knowledge, this approach has never been applied for numerical calculations of the structure or thermodynamics of one-site-associating fluids. Here we will show how a single simple approximation allows for the calculation

of N_{HB}. To approximate $Y_p(12)$ we note that this function can be decomposed into contributions from graphs that contain k association bonds F_{AA}

$$Y_p(12) = \sum_{k=0}^{\infty} Y_p^{(k)}(12) \tag{19}$$

The terms $Y_p^{(k)}$ give the contribution to Y_p from graphs that contain k association bonds. The simplest possible case is to keep only the first contribution $k=0$ and disregard all $Y_p^{(k)}$ for $k>0$. For this simple case

$$Y_p(12) = y_{ref}(12) \tag{20}$$

where y_{ref} is the cavity correlation function of the reference fluid, meaning association is treated as a perturbation to the reference fluid. This approximation is not necessarily intuitive since the structure of a fluid is expected to be strongly affected by association. Combining these results, the monomer fraction (fraction of molecules that do not have an association bond) can be written as

$$X_o = 1 - N_{NB} = \frac{-1 + \sqrt{1 + 4\Delta_{AA}}}{2\Delta_{AA}} \tag{21}$$

where Δ_{AA} is now given by $\Omega\Delta_{AA} = \rho \int y_{ref}(12)\, F_{AA}(12)\, d(2)$. Equation (21) gives a very simple relationship for the monomer fraction. This same equation was later derived by Chandler and Pratt [30] and Wertheim [22] using very different cluster expansions. Equation (21) has been shown to be highly accurate in comparison to simulation data [19, 34, 35]. Now we will introduce Wertheim's two-density formalism for one-site-associating fluids.

IV. SINGLE ASSOCIATION SITE: TWO-DENSITY APPROACH

In the previous section it was shown that Andersen's formalism can be applied to derive a highly accurate and simple relationship for the monomer fraction. In order to obtain this result the renormalized association Mayer functions $\tilde{F}_{AA}$ were employed. The applicability of Andersen's approach to more complex systems (mixtures, multiple bonds per association site, etc.) is limited by the fact that for each case the renormalized Mayer functions must be obtained by solving a rather complex combinatorial problem. A more natural formalism for describing association interactions in one-site-associating fluids is the two-density formalism of Wertheim [22, 31].

Instead of using the density expansion of the pair correlation function $g(12)$ or Helmholtz free energy A, Wertheim uses the fugacity expansion of $\ln \Xi$, where Ξ

is the grand partition function, as the starting point. Building on the ideas of Lockett [36], Wertheim then regroups the expansion such that individual graphs are composed of *s*-mer graphs. An *s*-mer represents a cluster of points that are connected by paths of F_{AA} bonds; each pair of points in an *s*-mer, which are not directly connected by a F_{AA} bond, receives an $e_{ref}(12)$ bond. This regrouping serves to include the geometry of association with the $e_{ref}(12)$ bonds enforcing the limited valence of the association interaction. In the *s*-mer representation, graphs that include unphysical core overlap are identically zero. That is, if the association site is singly bondable all graphs composed of *s*-mers of size $s>2$ immediately vanish due to steric hindrance. This is not the case in Andersen's approach where these unphysical contributions are allowed in individual graphs, with the single bonding condition being exploited with the *cancelation theorem*.

This regrouping of the fugacity expansion allows for the easy incorporation of steric effects. Now, unlike Andersen who tamed the arbitrarily large F_{AA} bonds through the introduction of a renormalized $\tilde{F}_{AA}$, Wertheim uses the idea of multiple densities, splitting the total density of the fluid as

$$\rho(1) = \rho_o(1) + \rho_b(1) \tag{22}$$

where $\rho_o(1)$ is the density of monomers (molecules not bonded) and $\rho_b(1)$ is the density of molecules that are bonded. The density $\rho_o(1)$ is composed of all graphs in $\rho(1)$ which do not have an incident F_{AA} bond, and $\rho_b(1)$ contains all graphs which have one or more incident F_{AA} bonds. Performing a topological reduction from fugacity graphs to graphs which contain $\rho_o(1)$ and $\rho(1)$ field points, allowed Wertheim to arrive at the following exact free energy

$$\frac{A}{k_B T} = \int \left(\rho(1) \ln\left(\rho_o(1) \Lambda^3 \right) - \rho_o(1) \right) d(1) - c^{(o)} \tag{23}$$

where for this case the graph sum $c^{(o)}$ is given as follows:

$$c^{(o)} = \left\{ \begin{array}{l} \text{sum of all irreducible graphs consisting of monomer points carrying} \\ \text{factors of } \rho, \text{ } s\text{-mer graphs with } s \geq 2 \text{ and every point carrying a factor} \\ \text{of } \rho_o, \text{ and } f_{ref}\text{-bonds between some sets of points in distinct } \textbf{\textit{s}}\text{-mers.} \end{array} \right\} \tag{24}$$

The first few graphs in the infinite series for $c^{(o)}$ are given in Fig. 4. In Fig. 4 crossed lines ⫞⫞⫞⫞⫞ represent F_{AA} bonds, dashed lines represent e_{ref} bonds, and solid lines represent f_{ref} bonds. All points with one or more incident F_{AA} bonds carry a factor $\rho_o(1)$, and each point with no incident F_{AA} bonds carries a factor $\rho(1)$. All graphs without any F_{AA} bonds (graphs **a**, **c**, **g**, **h**, and **i** in Fig. 4) represent

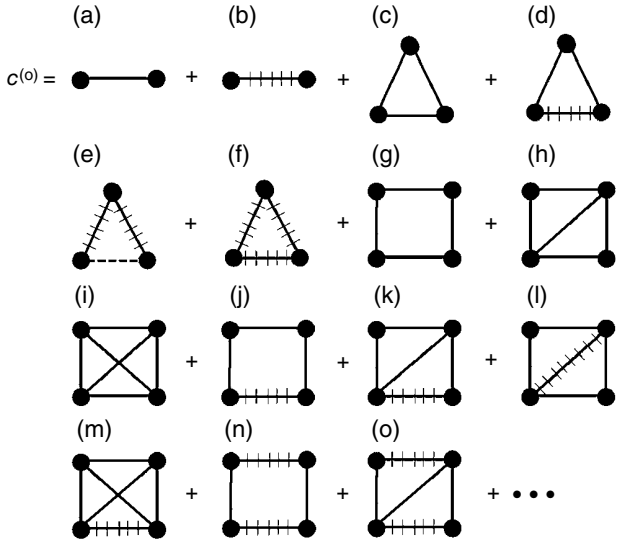

Figure 4. Graphical representation of Eq. (24) where crossed lines ⊣⊣⊣⊣⊣ represent F_{AA} bonds, dashed lines represent e_{ref} bonds, and solid lines represent f_{ref} bonds.

the reference system contribution $c_{ref}^{(o)}$. Any point that has two incident F_{AA} bonds (graphs **e** and **f** in fig. 4 are $s=3$-mers) represents a molecule with an association site which is bonded to two other molecules.

A. The Monovalent Case

If $\phi(12)$ is chosen such that the single bonding condition holds, then all s-mer graphs with $s>2$ vanish (e.g., graphs **e** and **f** in Fig. 4 are zero) and Eq. (24) can be summed exactly to yield the following:

$$c^{(o)} = c_{ref}^{(o)} + \frac{1}{2}\int \rho_o(1) f_{AA}(12) g_{oo}(12) \rho_o(2) d(1) d(2) \tag{25}$$

Note that Eq. (25) contains monomer densities since only monomers can associate. The use of monomer densities bounds the association term. The quantity $g_{oo}(12)$ is the monomer/monomer pair correlation function which can be ordered by graphs that contain k F_{AA} bonds:

$$g_{oo}(12) = \sum_{k=0}^{\infty} g_{oo}^{(k)}(12) \tag{26}$$

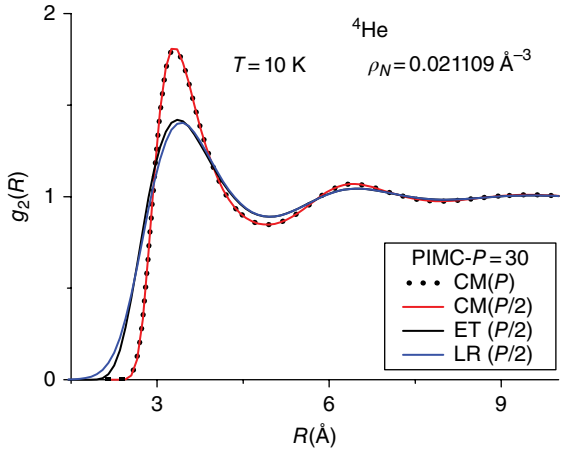

Figure 9. PIMC(AZS) pair radial correlation functions for fluid ^{4}He using the SCVJ propagator. CM(P) = global center of mass of the SCVJ necklaces. CM(P/2) = true centroid of the SCVJ necklaces. ET(P/2) = SCVJ instantaneous. LR(P/2) = SCVJ continuous linear response.

Chapter 3

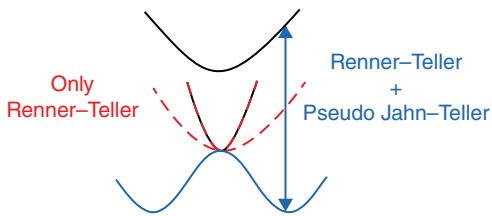

Figure 10. Illustration to the essential difference between the RTE and PJTE in application to linear systems in a twofold degenerate Π ground state: the RTE (dashed lines) splits the degenerate term and softens the lower state (hardening the upper one), whereas the PJTE (full lines), involving the interaction with the exited state (shown by arrow), may produce bending instability in the ground state (Reprinted with permission from Ref. 7. Copyright 2013, American Chemical Society).

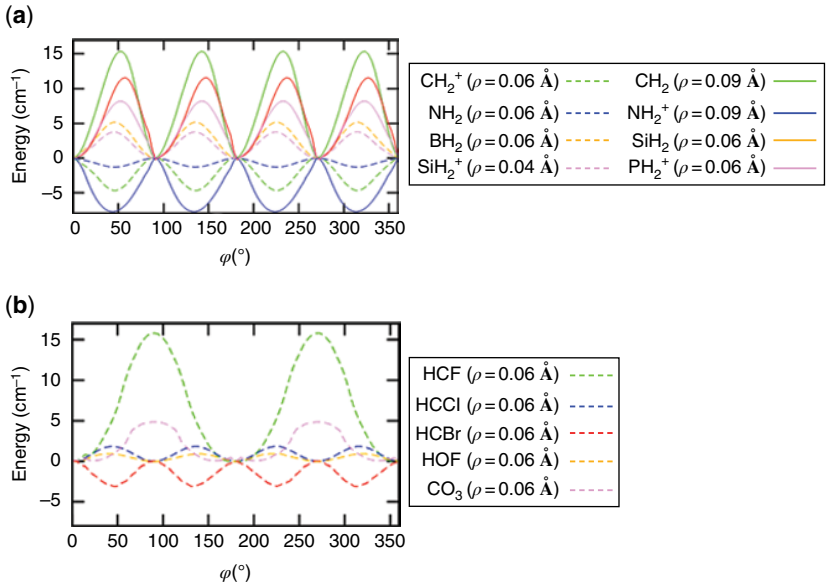

Figure 11. Potential energy profiles along the angle φ at a constant ρ value calculated by the CASSCF or SA-CASSCF method showing the amplitude of broken cylindrical symmetry in a series of linear triatomic molecules with $D_{\infty h}$ symmetry (**a**) and $C_{\infty v}$ symmetry (**b**) in the linear configuration (Reprinted with permission from Ref. 47. Copyright 2014, American Chemical Society).

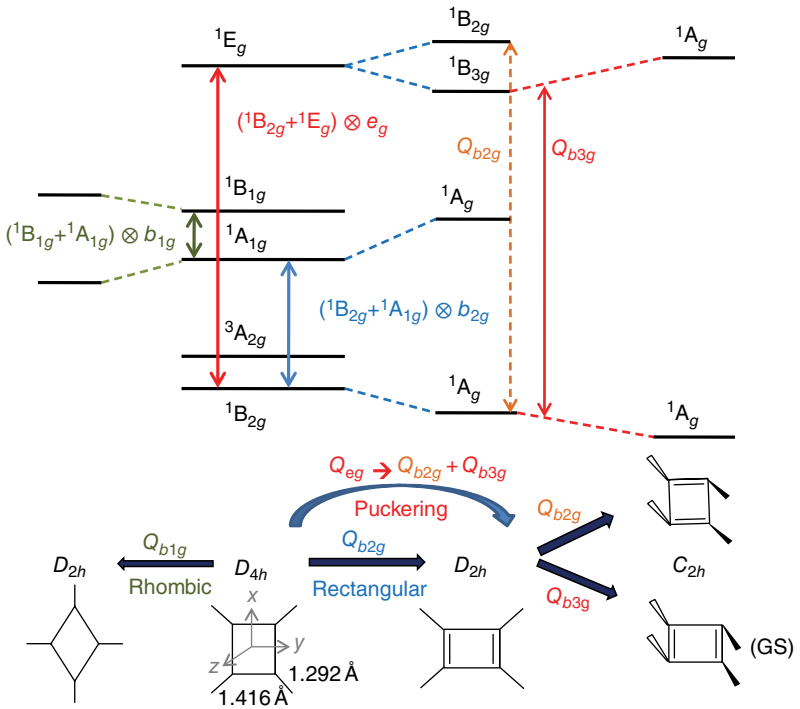

Figure 13. Electronic energy-level diagram of C_4F_4 showing the possible PJT couplings that result in corresponding distortions: the high-symmetry D_{4h} configuration may become rectangular D_{2h} (blue) due to the $(^1B_{2g}+^1A_{1g})\otimes b_{2g}$ coupling, and/or puckered (red) by coupling to higher excited E states, as well as rhombic (black) (GS denoted the ground state). The realization of any of these distortions or their combination is controlled by the PJTE criterion (11) (Reprinted with permission from Ref. 53. Copyright 2012, American Chemical Society).

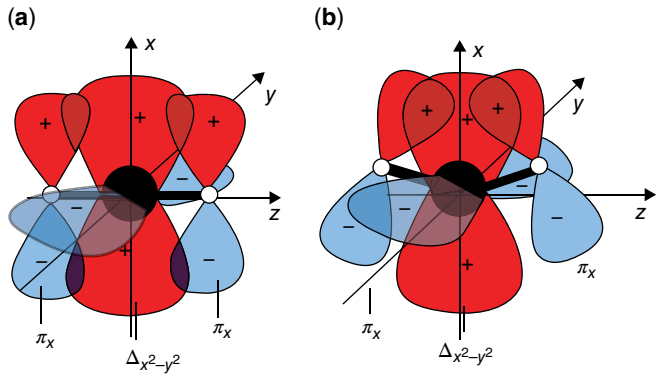

Figure 16. Illustration to the Δ_t – Π PJT interaction in a linear triatomic molecule producing added covalency by bending, and its fourfold symmetry: (**a**) In the linear configuration the Δ_{xy} and π_x orbitals of the corresponding terms as shown are orthogonal by symmetry (their total overlap is zero), and they don't participate in the bonding. (**b**) Upon bending, their overlap becomes nonzero resulting in additional covalence bonding that facilitates the bending. The angular dependence of the wavefunctions (π_x, π_y and Δ_{xy}, Δ_{x2-y2} for the Π and Δ_t terms, respectively) which are undefined in the degenerate states, becomes definitive after their splitting in the bent configuration, making their overlap periodical with a fourfold (for same marginal atoms) or twofold symmetry, (Reprinted with permission from Ref. 47. Copyright 2014, American Chemical Society).

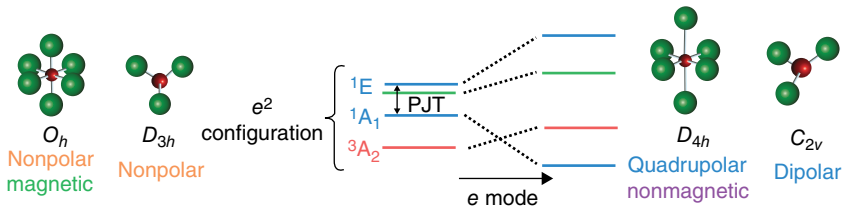

Figure 19. The e^2 electronic configuration spans the states $^3A_2$, $^1A_1$, and ^1E. While the magnetic $^3A_2$ state is lowest in energy and stable in the high-symmetry configuration (left), the $^1A_1$ and ^1E excited states interact via the PJTE, leading to a lower-energy nonmagnetic and distorted equilibrium configuration (right) (Reprinted with permission from Ref. 62. Copyright 2011, American Physical Society).

Chapter 5

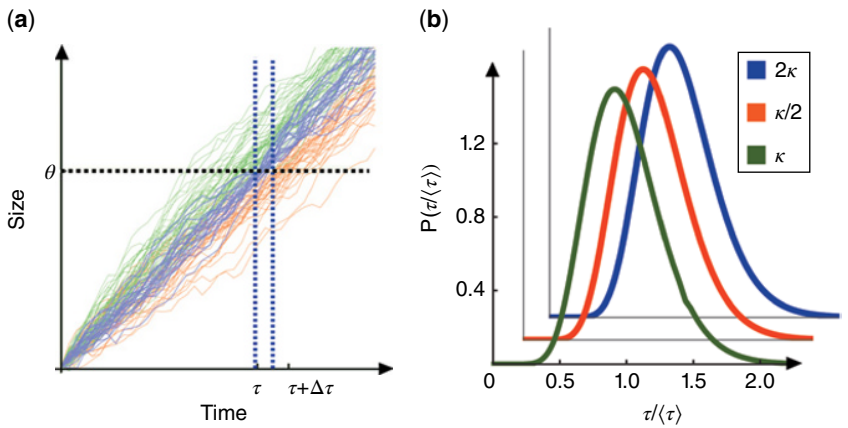

Figure 5. Cell division as a first-passage time (FPT) problem. (**a**) Schematic of stochastic cell size increase from a common initial condition. Between times τ and $\tau + \Delta\tau$, the some growth tracks cross the threshold size, θ. Using probability conservation, the cumulative probability that the size is greater than θ (above the black dotted horizontal line) must be equal to the complement of the cumulative probability that the FPT is less than or equal to τ (left of blue dotted vertical line at τ). (**b**) Scaling of the FPT distribution. The shape of the mean-rescaled division time distribution is timescale invariant, that is, independent of κ, when there is a single timescale, $1/\kappa \propto \tau$, in the FPT dynamics.